AGU ADVANCING EARTH AND SPACE SCIENCE

Geophysical Research Letters

RESEARCH LETTER
10.1029/2020GL090322

Control of Barents Sea Wintertime Cyclone Variability by Large-Scale Atmospheric Flow

Erica Madonna[1,2], Gabriel Hes[1,2,3], Camille Li[1,2], Clio Michel[1,2], and Peter Yu Feng Siew[1,2]

[1]Geophysical Institute, University of Bergen, Bergen, Norway, [2]Bjerknes Centre for Climate Research, Bergen, Norway, [3]Département de Géosciences, École Normale Supérieure, PSL Research University, Paris, France

Key Points:
- The temperature and moisture signature of cyclones depends on their origin and path more than their strength
- Jet stream and blocking play a primary role in the development and path of Arctic cyclones
- Arctic cyclone frequency exhibits large interannual variability and nonrobust trends

Supporting Information:
- Supporting Information S1

Correspondence to:
E. Madonna,
erica.madonna@uib.no

Citation:
Madonna, E., Hes, G., Li, C., Michel, C., & Siew, P. Y. F. (2020). Control of Barents Sea wintertime cyclone variability by large-scale atmospheric flow. *Geophysical Research Letters*, *47*, e2020GL090322. https://doi.org/10.1029/2020GL090322

Received 12 AUG 2020
Accepted 9 SEP 2020
Accepted article online 28 SEP 2020

Abstract Extratropical cyclones transport heat and moisture into the Arctic, which can promote surface warming and sea ice melt. We investigate wintertime cyclone variability in the Barents Sea region to understand what controls the impacts, frequency, and path of cyclones at high latitudes. Large-scale atmospheric conditions are found to be key, with the strongest surface warming from cyclones originating south of 60°N in the North Atlantic and steered northeastward by the upper-level flow. Atmospheric conditions also control cyclone variability in the Barents proper: Months with many cyclones are characterized by an absence of high-latitude blocking and enhanced local baroclinicity, due to the presence of strong upper-level winds and a southwest-northeast tilted jet stream more than changes in sea ice. This study confirms that Arctic cyclones exhibit large interannual variability, and accounting for this variability reveals that trends in Barents cyclone frequency are not robust over the 1979–2018 period.

Plain Language Summary Extratropical cyclones traveling from the midlatitudes can cause surface warming and sea ice melt upon reaching the Arctic. Focusing on the North Atlantic, this study aims to better understand what controls the number of cyclones reaching the Barents Sea, the differences in their climate impacts, and the exact paths they take on their journey northward. We find that cyclones originating south of 60°N produce the strongest Arctic warming. The large-scale atmospheric flow is key for steering the cyclones: more cyclones are found in the Barents Sea when the North Atlantic jet stream exhibits a pronounced southwest-northeast tilt, while fewer cyclones are found when quasi-stationary high-pressure systems, referred to as "blocking" systems, form at high latitudes. No remarkable differences in sea ice conditions seem to characterize periods with many/few cyclones in the Barents Sea. The winter-to-winter variability in the number of Arctic cyclones is large, and no robust trends are observed over the last 40 years.

1. Introduction

Extratropical cyclones play an important role in the global energy budget, redistributing heat and moisture from midlatitudes to high latitudes. In the North Atlantic sector, the bulk of the moisture and heat transport into the central Arctic is accomplished by transient eddies (Adams et al., 2000; Dufour et al., 2016; Peixoto & Oort, 1992; Sorteberg & Walsh, 2008) such as cyclones. Moisture entering the Arctic can enhance downward infrared radiation and lead to strong surface warming and sea ice melt (Boisvert et al., 2016; Messori et al., 2018; Woods et al., 2013), a process that is especially important in winter when insolation is weak. Moreover, winter cyclones can produce intense snowfall that acts as an insulation layer, modifying the melting and growth rates of sea ice (Graham et al., 2019). Cyclones with strong winds can influence the production and export of sea ice from the Arctic toward midlatitudes, with the export regions being sensitive to the cyclone's path (Brümmer et al., 2001; Rogers et al., 2005; Sorteberg & Kvingedal, 2006).

The surface impacts of cyclones entering the Arctic can vary widely from case to case. Already, several studies have shown that seasonal energy transport to the Arctic is dominated by a few specific transport events (Messori & Czaja, 2013; Moore, 2016), drawing attention to extreme Arctic cyclones (Koyama et al., 2017; Rinke et al., 2017; Sepp & Jaagus, 2011; Simmonds & Keay, 2009). For example, the passage of a single extreme cyclone is thought to be responsible for the unusual warmth of the entire 2015/2016 winter season (Boisvert et al., 2016; Kim et al., 2017; Moore, 2016). Extreme Arctic cyclones are often defined in terms of pressure or depth, but moisture content is likely as important, if not more, for surface impacts. Because the uptake and transport of moisture depend on a storm's formation and propagation environments

(e.g., Aemisegger & Papritz, 2018; Sodemann et al., 2008), discriminating between cyclones based on their origin and tracks should allow us to better evaluate their contribution to high-latitude climate variability.

The dynamics of storm tracks in midlatitude regions is well established, but there is some uncertainty about which environmental conditions are most important for controlling the development and path of cyclones at high latitudes. The common understanding is that cyclones are generated and grow in regions of enhanced baroclinicity in the presence of strong horizontal and vertical temperature gradients (Chang et al., 2002; Hoskins & Valdes, 1990; Shaw et al., 2016) and move on average eastward and poleward (Klein, 1958; Tamarin & Kaspi, 2016), steered by the large-scale flow. Some studies suggest that the large-scale flow also controls high-latitude cyclones through variability in the North Atlantic/Arctic Oscillation (Graversen, 2006; Simmonds et al., 2008) or the occurrence of blocking over the Ural Mountains (Luo et al., 2017). Other studies suggest that local conditions, such as the location of the sea ice edge, are a more important influence on the track of cyclones (Deser et al., 2000; Inoue et al., 2012). For example, Inoue et al. (2012) proposed that the retreat of Barents Sea ice weakens the local sea surface temperature gradient and thus the surface baroclincity. Consequently, cyclones tend not to travel east into the Barents Sea but rather turn north, resulting in a poleward shift of the storm track.

The Barents Sea is an ideal test bed for studying the effects of the large-scale flow versus local conditions on high-latitude cyclones. Situated at the end of the North Atlantic storm track (Chang et al., 2002; Shaw et al., 2016), the Barents Sea is one of the main corridors for cyclones entering the Arctic, in particular during winter (e.g., Adams et al., 2000; Simmonds et al., 2008; Sorteberg & Walsh, 2008). It is also the region with the largest wintertime sea ice variability (Parkinson et al., 1999; Parkinson & Cavalieri, 2008) and has experienced the strongest winter sea ice decline during the past decades (Onarheim et al., 2018; Stroeve & Notz, 2018; Vihma, 2014).

This study investigates wintertime cyclone variability in the Barents Sea, exploring the impacts of cyclones from different genesis regions as well as the roles of large-scale versus local conditions in determining cyclone tracks. A novel aspect of this study is that we document generalized relationships between the temperature and moisture signature of cyclones, their strength, and where they travel in their journey poleward. We also consider longer-term trends, accounting for cyclone origin and path, to provide a complementary view of regional differences in Arctic cyclones.

2. Data and Methods

We use the European Centre for Medium-Range Weather Forecasts reanalysis ERA-Interim (Dee et al., 2011) from 1979 to 2018 with 6-hourly time resolution and interpolated onto a $0.5 \times 0.5°$ spatial grid. Daily/monthly averages are generated as needed from the 6-hourly fields. Daily anomalies of 2-m temperature and moisture (vertically integrated from 1,000 to 100 hPa) are obtained by removing the monthly seasonal cycle and any linear trend from the total fields. We focus on winter (December, January, and February, DJF), the season with the strongest North Atlantic cyclone activity, and on the Barents Sea region, defined as 20–70°E longitude and 70–80°N latitude (see box in Figure 1).

2.1. PV Blocking

Atmospheric blocking is a persistent quasi-stationary high-pressure system that obstructs the westerly flow. Blocking extends through the whole troposphere and is characterized by low (or negative) potential vorticity (PV) values consistent with the anticyclonic circulation. In this study, blocking is detected using the approach of Schwierz et al. (2004), which identifies negative potential vorticity anomalies (−1.3 pvu, vertically averaged between 500 and 150 hPa) that persist for at least five consecutive days. This approach is particularly suitable for higher latitudes (poleward of 75°) as it can be applied to any area and does not require information from specific latitudinal bands to identify blocks (cf. geopotential height reversal; e.g., Scherrer et al., 2006). After identifying blocking from the 6-hourly data, monthly fields are obtained by averaging the number of blocked time steps at each grid point (Sprenger et al., 2017). A blocking climatology can be found in the supporting information (Figure S1). To calculate the blocking time series, we area-average the monthly blocking frequency over the Barents Sea region. Since there are 32 months with zero blocking density in the Barents Sea, no (high) blocking months are defined as the 32 months with zero (most frequent) blocking.

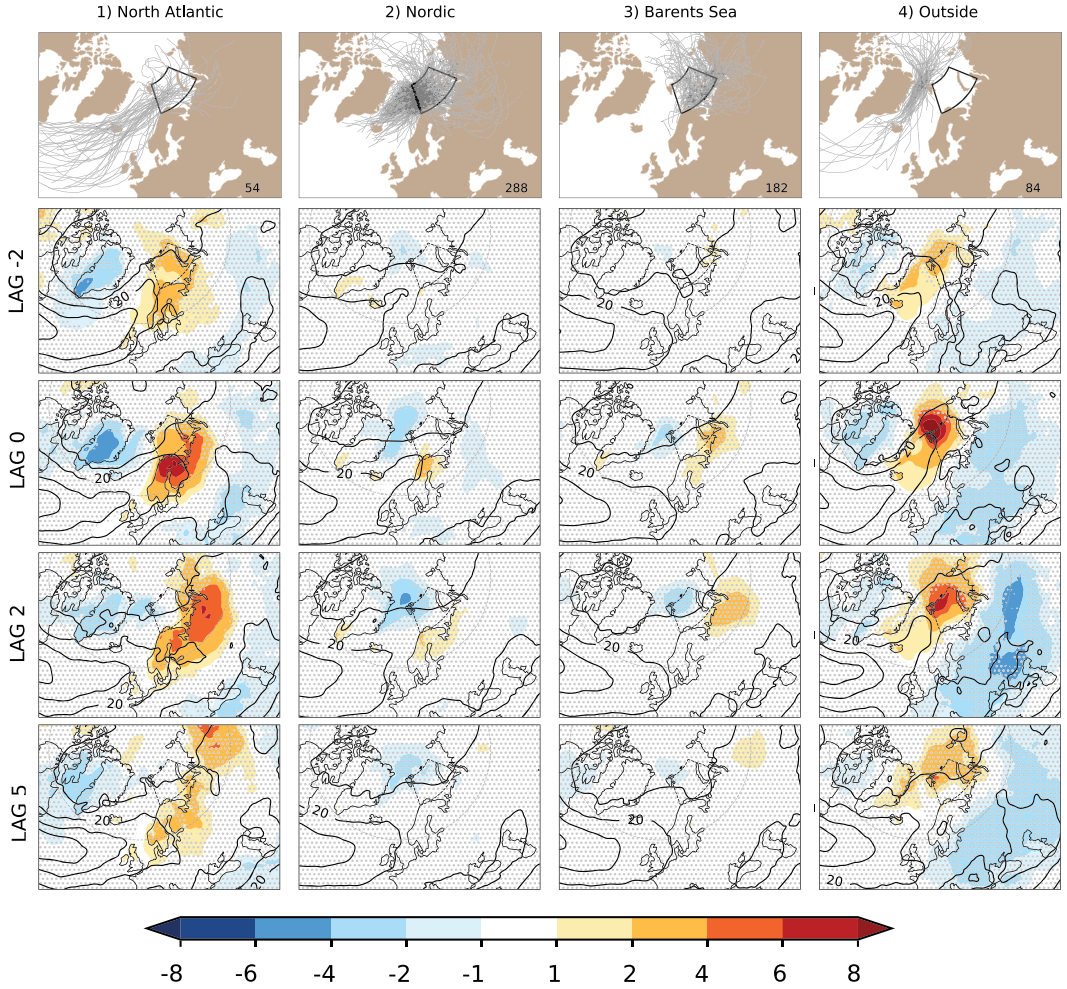

Figure 1. (first row) Cyclone tracks for the four cyclone categories (as defined in section 2.3): (1) North Atlantic, (2) Nordic, (3) Barents Sea, and (4) Outside. The total number of tracks for each category is shown at the bottom right corner of each panel, and the Barents Sea region is marked by the black box. (second to fifth rows) Composites of daily 2-m temperature anomalies (shading, in °C) and wind speed at 500 hPa (contours, starting at 15 m s^{-1}, 5 m s^{-1} intervals) shown at time lags −2, 0, 2, and 5 days. Lag 0 is defined for Categories 1–3 as the first time step when the track is in the Barents Sea box, while for Category 4 it is the first time step when the track is north of 80°N. Regions where the 0°C value lies within the 30th to 70th percentile range are marked with gray dots. The dashed gray circle marks the 60°N parallel.

2.2. Cyclone Identification

The Melbourne University algorithm detects and tracks maxima in the Laplacian of mean sea level pressure (MSLP) in space and time (Murray & Simmonds, 1991b, 1991a). We apply the algorithm on 6-hourly MSLP using the same parameters as Uotila et al. (2009). Only tracks lasting more than 2 days (nine track points) with genesis during DJF are kept. This excludes most polar lows and polar mesocyclones (Michel et al., 2018). From these tracks, we generate maps of monthly cyclone track densities (see climatology in Figure S1). Finally, we area-average the monthly track density over the Barents Sea region to produce a monthly time series of cyclone frequency. Similar to the PV blocking, we identify the 32 months with highest (lowest) cyclone density, hence frequent (infrequent) presence of cyclones in the Barents Sea. Simply counting the number of tracks entering the Barents Sea yields comparable results (Figure S2).

2.3. Cyclone Categories

We categorize the cyclone tracks based on their origins and paths (Figure 1, top row):

1. North Atlantic: cyclones entering the Barents Sea from the west with genesis south of 60°N (54 tracks)
2. Nordic: cyclones entering the Barents Sea from the west with genesis north of 60°N (288 tracks)

3. Barents Sea: cyclones with genesis in the Barents Sea (182 tracks)
4. Outside: cyclones traveling from the North Atlantic and crossing 80°N but not entering the Barents Sea (84 tracks)

The first three categories make up 74% of the total cyclone tracks present in the Barents Sea. Of the rest, most enter the Barents Sea from the south (16%), with a few entering from the north (6%) and east (4%). Since cyclones in all categories reach 70°N, we refer to them as Arctic cyclones. For the lag composites, Lag 0 is defined for Categories 1–3 as the first time step when the track is in the Barents Sea box, while for Category 4 it is the first time step when the track is north of 80°N. For the trend analysis, the number of tracks is aggregated for each winter, considering tracks starting between 1 December and 28 February.

2.4. Eady Growth Rate

To detect favorable conditions for cyclone development and growth, we compute the Eady growth rate (EGR). The EGR is a measure of lower-tropospheric baroclinicity (Hoskins & Valdes, 1990; Lindzen & Farrell, 1980), and it is defined as

$$\mathrm{EGR} = 0.31\frac{f}{N}\left\|\frac{d\mathbf{u}}{dZ}\right\| \tag{1}$$

with N, the Brunt-Väisälä frequency, defined as

$$N = \sqrt{\frac{g}{\theta_{700}}\frac{d\theta}{dZ}} \tag{2}$$

where f is the Coriolis parameter, g the gravitational acceleration, θ_{700} the potential temperature at 700 hPa, $d\mathbf{u}/dZ$ the vertical wind shear, and $d\theta/dZ$ the vertical gradient of potential temperature. The vertical gradients are evaluated using 6-hourly wind ($\mathbf{u}$), geopotential height (Z), and potential temperature (θ) at 850 and 500 hPa.

3. Results

The path traveled by a cyclone is of primary importance for its subsequent temperature impact on the Arctic. Composite analyses show that cyclones originating at lower latitudes (Category 1, Figure 1) are associated with stronger surface warming than cyclones originating at high latitudes (Categories 2 and 3). For cyclones from the North Atlantic that reach the Barents Sea (Category 1), we observe positive temperature (Figure 1, up to 8°C) and moisture (Figure S3, >2 g kg^{-1}) anomalies at Lag 0. The positive temperature anomaly persists for a few days (Lag 2) before diminishing (Lag 5). This warm anomaly is also present before the arrival of the cyclone in the Barents Sea (Lag −2), consistent with the southwest-northeast tilted jet stream (black contours) that advects warm and moist air from midlatitudes. The warm anomaly at Lag −2 is not linked to blocking, as none is detected at this time at high latitudes (Figure S4). The temperature and moisture anomalies associated with cyclones with genesis at higher latitudes (Category 2, Nordic and Category 3, Barents Sea) have smaller magnitude and spatial extent compared to Category 1. This is in line with the colder environment in which the cyclones form.

Cyclones forming in the North Atlantic traveling through the Fram Strait (Category 4) lead to comparable temperature and moisture anomalies as those entering the Barents Sea (Category 1). Here, the jet is strongly tilted as it is the case for Category 1, especially at Lag −2 and 0, which favors warm air advection. The main difference between Categories 1 and 4 is where the warming and moistening maximizes: over Scandinavia and northwest Russia for Category 1 and over the Barents Sea and Svalbard for Category 4. The shift in where the impacts maximize is related to the fact that the warm, moist anomalies are likely situated within the cyclone warm sector (cf. Wickström et al., 2019), while the cold, dry anomalies to the west result from cold air advection on the rear side of the cyclone (Papritz & Grams, 2018).

Since the location of strongest warming depends on the path of a cyclone, the large-scale flow must play a role in determining surface impacts. In the Barents Sea, there is a clear relationship between the presence of cyclones and an atmospheric pattern known as blocking, when a quasi-stationary and persistent high-pressure system diverts the mean westerly flow. A composite of months with high blocking (HB) frequency over the Barents Sea (Figure 2a) shows a reduction of cyclones locally and an increase in cyclones through the Fram Strait compared to a composite of months with no blocking (NB) in the Barents Sea

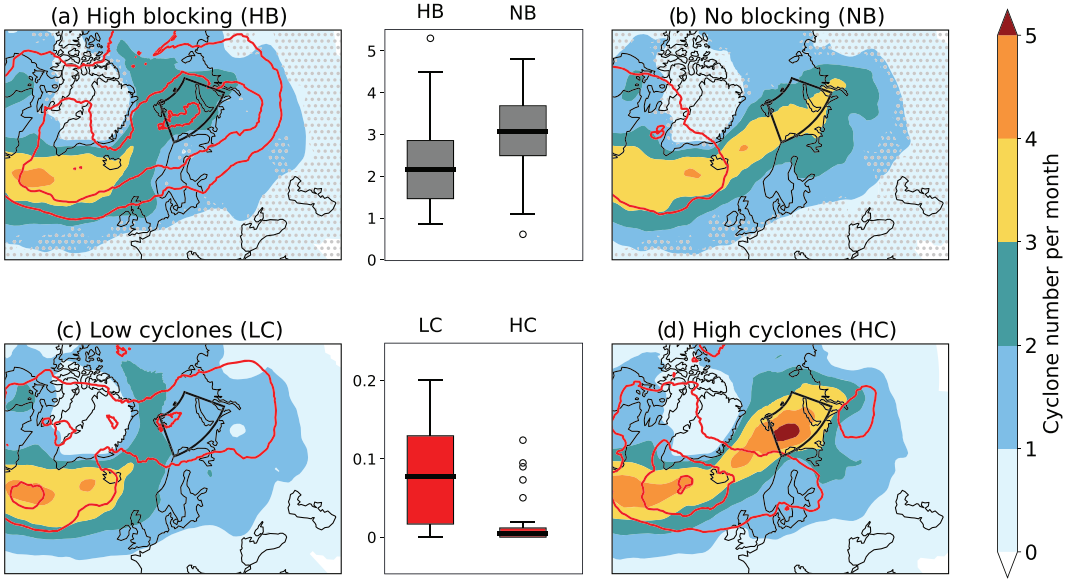

Figure 2. Composites of the number of cyclone tracks per month (shading) and PV blocking (red contours, as % of time, in 5% intervals) based on (a) high (HB) and (b) no (NB) blocking frequency and for (c) low (LC) and (d) high (HC) cyclone density in the Barents Sea. Dots in (a) and (b) mark regions where the mean composite cyclone density is less than its standard deviation (i.e., signal-to-noise ratio <1). The box-and-whisker plots show the distributions of cyclones (top, gray) and blocking (bottom, red) frequencies averaged over the Barents Sea region (black box) for the 32 months used in each composite. The black horizontal line shows the median, boxes show the interquartile range (IQR), and whiskers represent the median ± 1.5 IQR.

(Figure 2b). The mean cyclone track density averaged over the Barents Sea area is 2.3 (3.0) tracks per month for high (no) blocking months (Figures 2a and 2b, boxplot). The composites show comparably large month-to-month variability, evident from the overlapping ranges in the HB/NB box-and-whisker plot. Still, the composite means over the considered regions are larger than their standard deviations (dots in Figures 2a and 2b indicate signal-to-noise ratio <1). The link between Barents Sea cyclones and the occurrence of high-latitude blocking is consistent with findings from previous studies that show more cyclones passing through the Fram Strait when there is a high-pressure ridge over Scandinavia (Michel et al., 2012; Wickström et al., 2019).

An inverse analysis produces consistent results: months with a low occurrence of cyclones (LC) in the Barents Sea are associated with blocking over the Barents Sea (Figure 2c, red contours and boxplot) and also more cyclones entering the Arctic through the Fram Strait. In addition, months with a high occurrence of cyclones (HC) in the Barents Sea show less frequent blocking over the region (Figure 2d), similar to the NB composite (Figure 2b). One notable difference is that the HC composite exhibits enhanced cyclone frequency over the whole North Atlantic compared to the NB composite. This suggests that the number of cyclones entering the Barents Sea depends not only on large-scale atmospheric blocking but also on upstream conditions of the North Atlantic storm track.

Previous studies have linked cyclone variability in the Arctic to changes in baroclinicity (Inoue et al., 2012; Koyama et al., 2017; Wickström et al., 2019), with one specific suggestion that sea ice retreat decreases baroclinicity locally and prevents cyclones from the North Atlantic or Nordic Seas from traveling eastward into the Barents Sea. To test the influence of sea ice on cyclone variability in the Barents Sea region, we examine composites of the EGR and sea ice area for months with high (HC) and low (LC) cyclone frequency in the Barents Sea (i.e., the same months as in Figures 2d and 2c). The high cyclone composite shows higher EGR values over the Barents Sea than the low-cyclone composite (Figure 3, first column). However, there are almost no differences in the location of the sea ice edge between the two composites (blue and red lines). Moreover, the EGR signals are not confined to the Barents Sea but extend to the Nordic Seas. We see that the differences in the EGR mainly result from differences in the vertical wind shear (second column), which are linked to large-scale flow features such as the extension and tilt of the upper-level jet (third column). Similar conclusions can be drawn by compositing based on blocking frequency (Figure S5) rather than cyclone

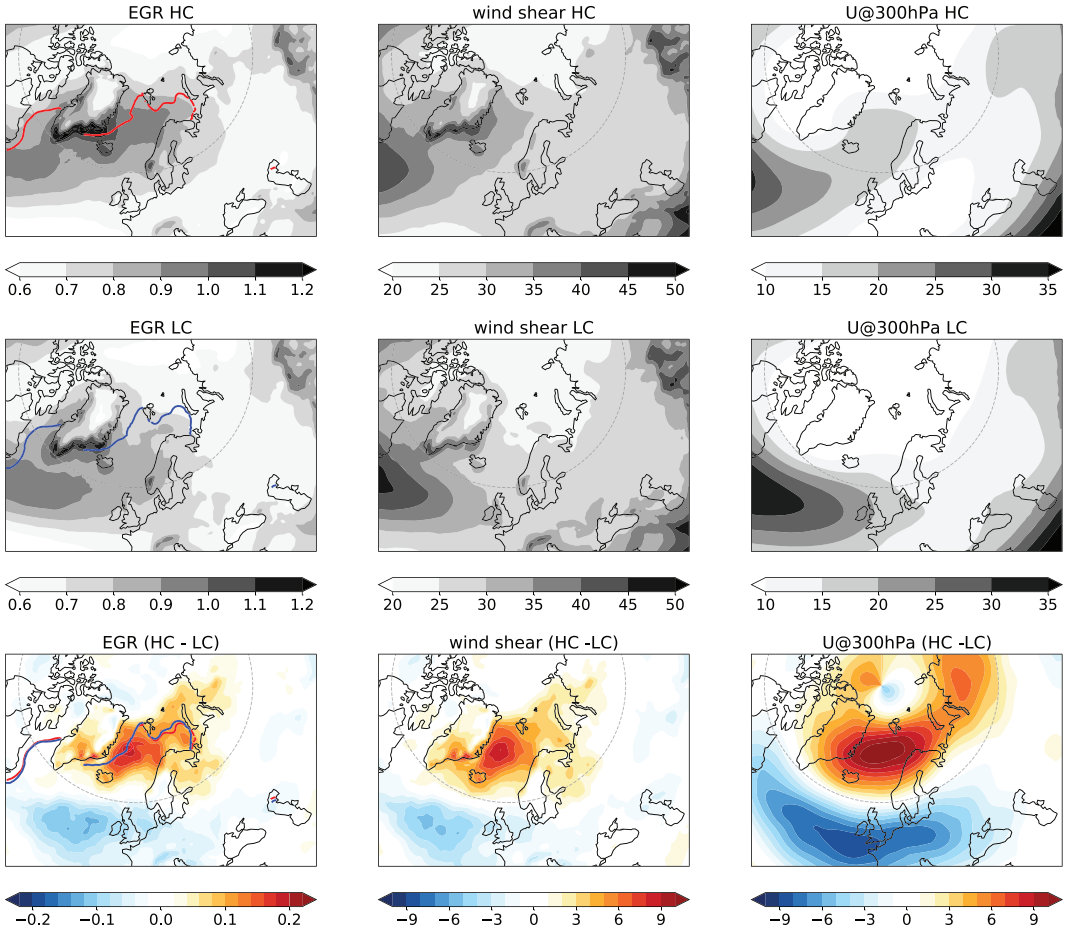

Figure 3. Composites of Eady growth rate (EGR, in day^{-1}), wind shear between 500 and 850 hPa (in 10^{-4} s^{-1}) and zonal wind at 300 hPa (U, in m s^{-1}) for high-cyclone-frequency months (HC, first row), low-cyclone-frequency months (LC, second row), and their difference (HC − LC, third row). The red (blue) line shows the ice edge (0.15 sea ice area fraction, undetrended data) for the HC (LC) composite. The dashed gray circle marks the 60°N parallel.

frequency. The role of the jet stream in setting favorable conditions for cyclone development is also visible when considering cyclone categories separately. Regions with enhanced EGR are systematically located on the poleward side of the jet stream (Figure S4) and are observed before the cyclones reach the Arctic (i.e., at Lag −2, Figure S4).

The key elements identified in the composite analysis, including the role of atmospheric blocking, are supported by a case study from the 2015/2016 winter. This winter season saw a major Arctic warming event, with some regions north of Svalbard registering daily temperatures of 30°C above the wintertime climatology (Binder et al., 2017; Boisvert et al., 2016; Kim et al., 2017; Moore, 2016). From 24 to 27 December, prior to the warming event, several cyclones (Figure 4, blue shading) enter or are formed in the Barents Sea. On 27 December, a block (red contours) forms north of Iceland and grows, migrating to a position over the Barents Sea by 29 December. The block persists for the next 6 days and is associated with a high-pressure system at the surface (gray shading). During this time (29 December to 4 January) no cyclones enter the domain, and cyclones traveling from the North Atlantic instead enter the Arctic through Fram Strait, most of them accompanied by a strong upper-level jet (Figure S6). The cyclone entering the Fram Strait on 31 December, marked by a blue cross in Figure 4, transported an extremely warm and humid air mass into the Arctic (Boisvert et al., 2016; Moore, 2016) and likely contributed to the localized thinning of sea ice over the Barents-Kara Seas region (Binder et al., 2017; Boisvert et al., 2016). Despite the reduction in sea ice thickness, the location of the sea ice edge (white contour), which may influence the low-level baroclinicity, did not change substantially during the 10-day warming event. Regions with high EGR values (purple contours in Figure S6) mainly coincide with strong upper-level winds.

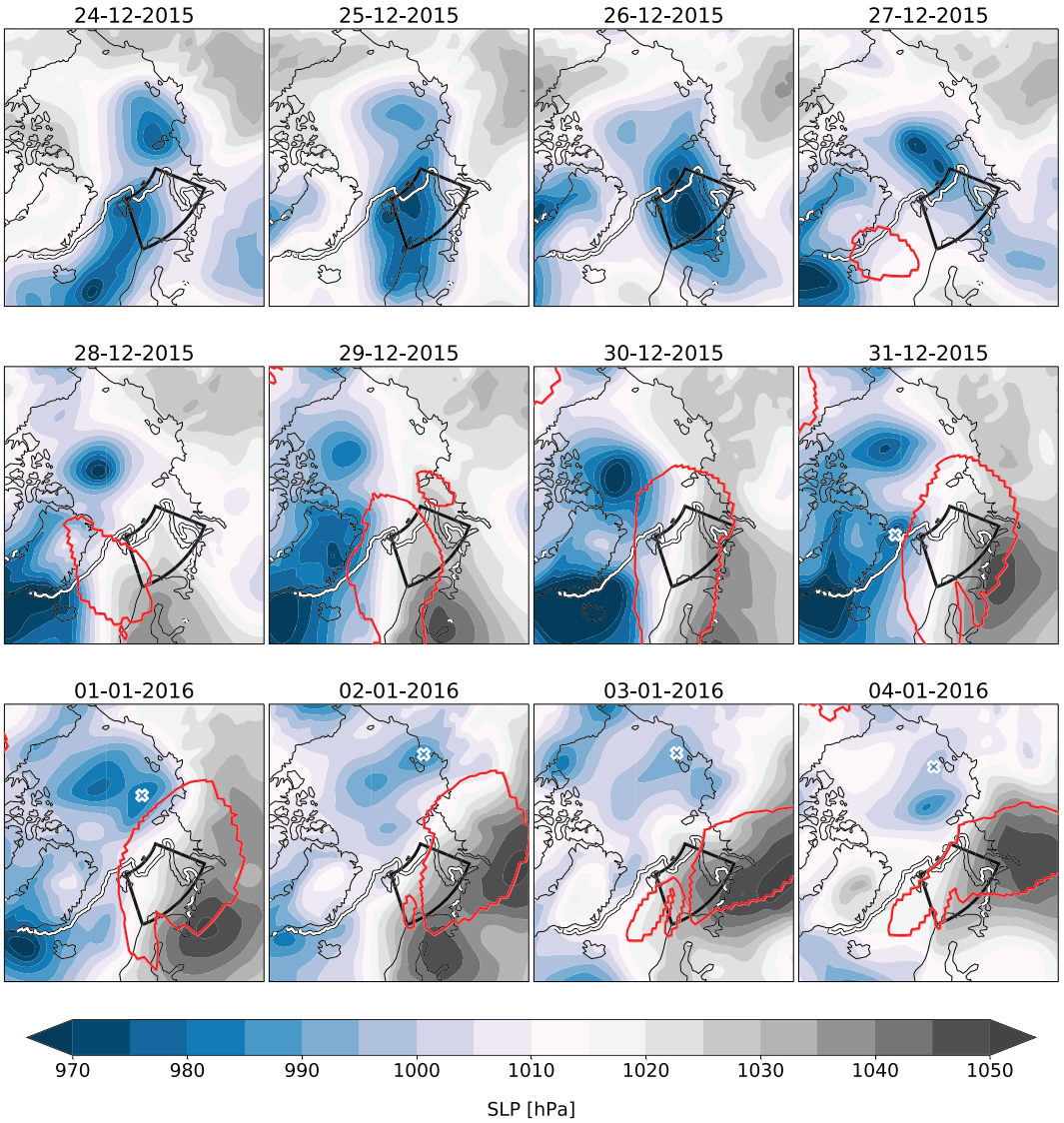

Figure 4. Temporal evolution of mean sea level pressure (MSLP in hPa, shading), sea ice edge (white line showing 0.15 ice area fraction), and blocked area (enclosed by red contours) at 12 UTC from 24 December 2015 to 4 January 2016. The black box delimits the Barents Sea region, while the blue cross marks the cyclone described in Boisvert et al. (2016).

4. Discussion

We have examined cyclone variability in the Barents Sea and demonstrated links to the large-scale atmospheric conditions. We have also shown that variability in cyclone frequency and baroclinicity in the Barents Sea reflect variability in the upper-level flow more than the sea ice edge. Under global warming scenarios, models studies suggest that the melting of sea ice might impact the atmospheric circulation (e.g., Butler et al., 2010; Zappa et al., 2018). Given the notable retreat of winter sea ice in the Barents Sea over recent decades, it is natural to ask if this region exhibits long-term changes in cyclones.

We find no robust trends in cyclone frequency in any of the considered categories (Figure 5). This result is at odds with recent studies that reported a decrease in cyclone frequency in the southeastern Barents Sea during winter (Rinke et al., 2017; Wickström et al., 2019; Zahn et al., 2018). The discrepancy arises in part from differences in the cyclone tracking schemes or data sets used but mostly from how significance of trends is evaluated. In addition to using a *t* test, we also use a Theil-Sen estimator, a method that is insensitive to outliers and more appropriate for short, noisy records. The time series of the number of winter (DJF) cyclones

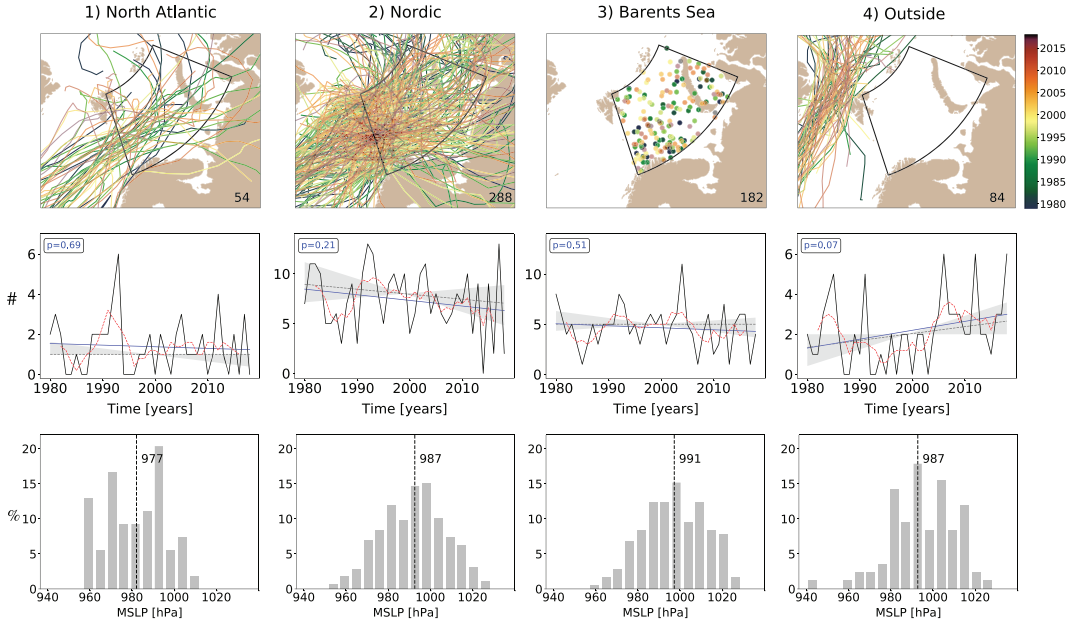

Figure 5. Spatial distribution of cyclone tracks (first row), time series of the number of cyclone tracks (second row), and MSLP at Lag 0 (third row) for the four categories as defined in section 2.3 during DJF winter. (first row) For cyclones with genesis in the Barents Sea (Category 3), cyclogenesis locations are shown instead of cyclone tracks. Both track and genesis locations are color coded by year. The total number of tracks in each category is shown at the bottom right corner of each panel. (second row) Linear regression slopes (p value in the top left corner) are shown in blue. Theil-Sen median slope is shown in gray (dashed line), and the corresponding 95% confidence interval is indicated by the gray shading. A five-winter moving average is shown in red (dashed line). Year labels correspond to the January and February, such that 1980 is the winter season from December 1979 to February 1980. (third row) Histograms of MSLP (normalized frequency in %) at Lag 0 for the four categories. Median value (in hPa) is shown by the black dashed line.

entering the Barents Sea (Categories 1–3, Figure 5) show large interannual variability, with weakly negative but nonsignificant trends based on both the t test (using a standard significance level of 0.05) and the Theil-Sen test (uncertainty range includes both positive and negative slopes). Applying a five-winter running mean (red lines) does not reveal any particular cyclic behavior. Considering Categories 1–3 together confirms the general picture of a slight and nonsignificant decrease in cyclones in the Barents Sea (not shown). These results agree with the studies of Koyama et al. (2017), who found no link between changes in cyclone frequency and sea ice loss, and Vessey et al. (2020), who found no trend in winter Arctic cyclone frequency and characteristics. The "Outside" category shows a positive but nonrobust trend in cyclone frequency.

In addition to the number of cyclones, the path of cyclones also shows large interannual variability. Inoue et al. (2012) suggested that cyclone tracks shift northward as sea ice retreats. Such a northward (or more generally, poleward) shift is expected under global warming (Harvey et al., 2014; Shaw et al., 2016; Tamarin-Brodsky & Kaspi, 2017; Yin, 2005), but most of the proposed mechanisms involve changes in the upper-level temperature gradient. Whether such changes are already detectable in the observational period is questionable. We do not observe any clear poleward shift of cyclone tracks with time (Figure 5, colored tracks, first row), consistent with the results of Koyama et al. (2017). Furthermore, for cyclones with genesis in the Barents Sea (Figure 5), the spatial distribution shows no systematic shift over the last four decades.

Wickström et al. (2019) suggested that decreasing cyclone frequency in the Barents Sea is linked to changes in the large-scale flow. They documented an increase in the frequency of the Scandinavian pattern, an anticyclonic circulation anomaly over Scandinavia and western Russia. This pattern might be linked to Barents Sea blocking, which we showed to be important for determining the path of cyclones. There is an apparent increase in the blocking time series, but again this trend is not robust over the observational period (Figure S7). The other pattern of interest in this region is the North Atlantic Oscillation (NAO). As expected, when the NAO is positive the jet stream has a strong southwest-northeast tilt, steering more cyclones toward the high latitudes (Figure S8). However, the NAO index and frequency of cyclones is poorly correlated (correlations below 0.4) for all categories, on both seasonal and monthly time scales (Figure S8).

Cyclones with the strongest surface warming are not necessarily the most extremes. Extreme cyclones are often defined using a MSLP threshold (Chang et al., 2012; Rinke et al., 2017; Vavrus, 2013). Figure 5 (third row) shows cyclone MSLP at Lag 0 for the four Arctic cyclone categories. Each category exhibits large variability in MSLP. The North Atlantic cyclones have lower MSLP values (median of 977 hPa) than the others. Outside cyclones have the same MSLP median (987 hPa) as the Nordic but show much stronger temperature and moisture anomalies (cf. Lag 0 in Figures 1 and S3). This suggests that not all cyclones producing strong surface warming are extreme in MSLP.

Cyclones are just one of several phenomena that give rise to sea ice variability in the Barents Sea. The impact of cyclones on sea ice depends on their characteristics and spans from surface warming to mechanical ice breakup (Graham et al., 2019). Other factors influencing wintertime sea ice variability are the inflow of warm Atlantic water into the Barents Sea driven by local wind forcing (e.g., Akperov et al., 2020; Alexeev et al., 2017; Årthun et al., 2012; Smedsrud et al., 2013), as well as the preconditions at the end of the melting season. Also, marine cold air outbreaks (Papritz, 2020) and high-latitude blocking (Gong & Luo, 2017; Papritz, 2020; Pfahl & Wernli, 2012) influence Arctic temperatures.

5. Conclusions

In this study, we investigate Arctic cyclones to understand what influences variability in their frequency, path, and impacts. Surface warming associated with Arctic cyclones depends not only on their strength (Figure 5) but most importantly on their origin and the path they take toward the Arctic (Figure 1). The path of Arctic cyclones is controlled by the large-scale flow, just as for midlatitude cyclones. The upper-level jet is more important than sea ice for enhancing baroclinicity and creating favorable conditions for cyclone growth (Figure 3). Cyclones travel north through the Fram Strait when there is blocking over the Barents Sea (Figures 2 and 4). Interannual variability is large for all Arctic cyclone categories, and no robust trends in frequency are observed (Figure 5). While a single extreme cyclone can affect sea ice cover, the link on seasonal and longer time scales is more complicated and might change with global warming as sea ice thins and easily breaks up and drifts.

Data Availability Statement

The ERA-Interim reanalysis is freely available online (at https://apps.ecmwf.int/datasets/data/interim-full-daily/levtype=pl/).

Acknowledgments
We acknowledge the ECMWF for providing the ERA-Interim reanalysis. The authors would like to thank the atmospheric dynamics group at ETH Zürich for providing the blocking detection as well as Melbourne University for making their cyclone detection and tracking algorithm available. The authors are grateful to Lukas Papritz and Paul Kushner for fruitful discussions during early stages of the study. We thank two anonymous reviewers for their comments that helped improve and clarify this manuscript. This work was supported by funding from the Research Council of Norway (Nansen Legacy grant 276730 and DynAMiTe grant 255027).

References

Adams, J. M., Bond, N. A., & Overland, J. E. (2000). Regional variability of the Arctic heat budget in fall and winter. *Journal of Climate*, *13*(19), 3500–3510.

Aemisegger, F., & Papritz, L. (2018). A climatology of strong large-scale ocean evaporation events. Part I: Identification, global distribution, and associated climate conditions. *Journal of Climate*, *31*(18), 7287–7312.

Akperov, M., Semenov, V. A., Mokhov, I. I., Dorn, W., & Rinke, A. (2020). Impact of Atlantic water inflow on winter cyclone activity in the Barents Sea: Insights from coupled regional climate model simulations. *Environmental Research Letters*, *15*(2), 024009.

Alexeev, V. A., Walsh, J. E., Ivanov, V. V., Semenov, V. A., & Smirnov, A. V. (2017). Warming in the Nordic Seas, North Atlantic storms and thinning Arctic sea ice. *Environmental Research Letters*, *12*(8), 084011.

Årthun, M., Eldevik, T., Smedsrud, L. H., Skagseth, O., & Ingvaldsen, R. B. (2012). Quantifying the influence of Atlantic heat on Barents Sea ice variability and retreat. *Journal of Climate*, *25*(13), 4736–4743.

Binder, H., Boettcher, M., Grams, C. M., Joos, H., Pfahl, S., & Wernli, H. (2017). Exceptional air mass transport and dynamical drivers of an extreme wintertime Arctic warm event. *Geophysical Research Letters*, *44*, 12,028–12,036. https://doi.org/10.1002/2017GL075841

Boisvert, L. N., Petty, A. A., & Stroeve, J. C. (2016). The impact of the extreme winter 2015/16 Arctic cyclone on the Barents–Kara Seas. *Monthly Weather Review*, *144*(11), 4279–4287.

Brümmer, B., Müller, G., Affeld, B., Gerdes, R., Karcher, M., & Kauker, F. (2001). Cyclones over Fram Strait: Impact on sea ice and variability. *Polar Research*, *20*(2), 147–152.

Butler, A. H., Thompson, D. W. J., & Heikes, R. (2010). The steady-state atmospheric circulation response to climate change-like thermal forcings in a simple general circulation model. *Journal of Climate*, *23*(13), 3474–3496.

Chang, E. K. M., Guo, Y., & Xia, X. (2012). CMIP5 multimodel ensemble projection of storm track change under global warming. *Journal of Geophysical Research*, *117*, D23118. https://doi.org/10.1029/2012JD018578

Chang, E. K. M., Lee, S., & Swanson, K. L. (2002). Storm track dynamics. *Journal of Climate*, *15*(16), 2163–2183.

Dee, D. P., Uppala, S. M., Simmons, A. J., Berrisford, P., Poli, P., Kobayashi, S., et al. (2011). The ERA-Interim reanalysis: Configuration and performance of the data assimilation system. *Quarterly Journal of the Royal Meteorological Society*, *137*(656), 553–597.

Deser, C., Walsh, J. E., & Timlin, M. S. (2000). Arctic sea ice variability in the context of recent atmospheric circulation trends. *Journal of Climate*, *13*(3), 617–633.

Dufour, A., Zolina, O., & Gulev, S. K. (2016). Atmospheric moisture transport to the Arctic: Assessment of reanalyses and analysis of transport components. *Journal of Climate*, *29*(14), 5061–5081.

Gong, T., & Luo, D. (2017). Ural blocking as an amplifier of the Arctic sea ice decline in winter. *Journal of Climate*, *30*(7), 2639–2654.
Graham, R. M., Itkin, P., Meyer, A., Sundfjord, A., Spreen, G., Smedsrud, L. H., et al. (2019). Winter storms accelerate the demise of sea ice in the Atlantic sector of the Arctic Ocean. *Scientific Reports*, *9*(1), 1–16.
Graversen, R. G. (2006). Do changes in the midlatitude circulation have any impact on the Arctic surface air temperature trend? *Journal of Climate*, *19*(20), 5422–5438.
Harvey, B. J., Shaffrey, L. C., & Woollings, T. J. (2014). Equator-to-pole temperature differences and the extra-tropical storm track responses of the CMIP5 climate models. *Climate Dynamics*, *43*(5–6), 1171–1182.
Hoskins, B. J., & Valdes, P. J. (1990). On the existence of storm-tracks. *Journal of the Atmospheric Sciences*, *47*(15), 1854–1864.
Inoue, J., Hori, M. E., & Takaya, K. (2012). The role of Barents Sea ice in the wintertime cyclone track and emergence of a warm-Arctic cold-Siberian anomaly. *Journal of Climate*, *25*, 2561–2568.
Kim, B.-M., Hong, J.-Y., Jun, S.-Y., Zhang, X., Kwon, H., Kim, S.-J., et al. (2017). Major cause of unprecedented Arctic warming in January 2016: Critical role of an Atlantic windstorm. *Scientific Reports*, *7*(1), 1–9.
Klein, W. H. (1958). The frequency of cyclones and anticyclones in relation to the mean circulation. *Journal of Meteorology*, *15*(1), 98–102.
Koyama, T., Stroeve, J., Cassano, J., & Crawford, A. (2017). Sea ice loss and Arctic cyclone activity from 1979 to 2014. *Journal of Climate*, *30*(12), 4735–4754.
Lindzen, R. S., & Farrell, B. (1980). A simple approximate result for the maximum growth rate of baroclinic instabilities. *Journal of the Atmospheric Sciences*, *37*(7), 1648–1654. https://doi.org/10.1175/1520-0469(1980)037<1648:ASARFT>2.0.CO;2
Luo, B., Luo, D., Wu, L., Zhong, L., & Simmonds, I. (2017). Atmospheric circulation patterns which promote winter Arctic sea ice decline. *Environmental Research Letters*, *12*(5), 054017. https://doi.org/10.1088/1748-9326/aa69d0
Messori, G., & Czaja, A. (2013). On the sporadic nature of meridional heat transport by transient eddies. *Quarterly Journal of the Royal Meteorological Society*, *139*(673), 999–1008.
Messori, G., Woods, C., & Caballero, R. (2018). On the drivers of wintertime temperature extremes in the high Arctic. *Journal of Climate*, *31*(4), 1597–1618.
Michel, C., Rivière, G., Terray, L., & Joly, B. (2012). The dynamical link between surface cyclones, upper-tropospheric Rossby wave breaking and the life cycle of the Scandinavian blocking. *Geophysical Research Letters*, *39*, L10806. https://doi.org/10.1029/2012GL051682
Michel, C., Terpstra, A., & Spengler, T. (2018). Polar mesoscale cyclone climatology for the Nordic Seas based on ERA-Interim. *Journal of Climate*, *31*, 2511–2532.
Moore, G. W. K. (2016). The December 2015 North Pole warming event and the increasing occurrence of such events. *Scientific Reports*, *6*, 39084.
Murray, R. J., & Simmonds, I. (1991a). A numerical scheme for tracking cyclone centres from digital data. Part II: Application to January and July general circulation model simulations. *Australian Meteorological Magazine*, *39*, 167–180.
Murray, R. J., & Simmonds, I. (1991b). A numerical scheme for tracking cyclone centres from digital data. Part I: Development and operation of the scheme. *Australian Meteorological Magazine*, *39*, 155–166.
Onarheim, I. H., Eldevik, T., Smedsrud, L. H., & Stroeve, J. C. (2018). Seasonal and regional manifestation of Arctic sea ice loss. *Journal of Climate*, *31*(12), 4917–4932.
Papritz, L. (2020). Arctic lower-tropospheric warm and cold extremes: Horizontal and vertical transport, diabatic processes, and linkage to synoptic circulation features. *Journal of Climate*, *33*(3), 993–1016.
Papritz, L., & Grams, C. M. (2018). Linking low-frequency large-scale circulation patterns to cold air outbreak formation in the northeastern North Atlantic. *Geophysical Research Letters*, *45*, 2542–2553. https://doi.org/10.1002/2017GL076921
Parkinson, C. L., & Cavalieri, D. J. (2008). Arctic sea ice variability and trends, 1979–2006. *Journal of Geophysical Research*, *113*, C07003. https://doi.org/10.1029/2007JC004558
Parkinson, C. L., Cavalieri, D. J., Gloersen, P., Zwally, H. J., & Comiso, J. C. (1999). Arctic sea ice extents, areas, and trends, 1978–1996. *Journal of Geophysical Research*, *104*(C9), 20,837–20,856.
Peixoto, J. P., & Oort, A. H. (1992). *Physics of climate*. New York, NY (United States): American Institute of Physics.
Pfahl, S., & Wernli, H. (2012). Quantifying the relevance of atmospheric blocking for co-located temperature extremes in the Northern Hemisphere on (sub-) daily time scales. *Geophysical Research Letters*, *39*, L12807. https://doi.org/10.1029/2012GL052261
Rinke, A., Maturilli, M., Graham, R. M., Matthes, H., Handorf, D., Cohen, L., et al. (2017). Extreme cyclone events in the Arctic: Wintertime variability and trends. *Environmental Research Letters*, *12*, 094006. https://doi.org/10.1088/1748-9326/aa7def
Rogers, J. C., Yang, L., & Li, L. (2005). The role of Fram Strait winter cyclones on sea ice flux and on Spitsbergen air temperatures. *Geophysical Research Letters*, *32*, L06709. https://doi.org/10.1029/2004GL022262
Scherrer, S. C., Croci-Maspoli, M., Schwierz, C., & Appenzeller, C. (2006). Two-dimensional indices of atmospheric blocking and their statistical relationship with winter climate patterns in the Euro-Atlantic region. *International Journal of Climatology*, *26*, 233–249.
Schwierz, C., Croci-Maspoli, M., & Davies, H. C. (2004). Perspicacious indicators of atmospheric blocking. *Geophysical Research Letters*, *31*, L06125. https://doi.org/10.1029/2003GL019341
Sepp, M., & Jaagus, J. (2011). Changes in the activity and tracks of Arctic cyclones. *Climatic Change*, *105*(3-4), 577–595. https://doi.org/10.1007/s10584-010-9893-7
Shaw, T. A., Baldwin, M., Barnes, E. A., Caballero, R., Garfinkel, C. I., Hwang, Y.-T., et al. (2016). Storm track processes and the opposing influences of climate change. *Nature Geoscience*, *9*(9), 656–664.
Simmonds, I., Burke, C., & Keay, K. (2008). Arctic climate change as manifest in cyclone behavior. *Journal of Climate*, *21*(22), 5777–5796.
Simmonds, I., & Keay, K. (2009). Extraordinary September Arctic sea ice reductions and their relationships with storm behavior over 1979–2008. *Geophysical Research Letters*, *36*, L19715. https://doi.org/10.1029/2009GL039810
Smedsrud, L. H., Esau, I., Ingvaldsen, R. B., Eldevik, T., Haugan, P. M., Li, C., et al. (2013). The role of the Barents Sea in the Arctic climate system. *Reviews of Geophysics*, *51*, 415–449. https://doi.org/10.1002/rog.20017
Sodemann, H., Schwierz, C., & Wernli, H. (2008). Interannual variability of Greenland winter precipitation sources: Lagrangian moisture diagnostic and North Atlantic Oscillation influence. *Journal of Geophysical Research*, *113*, D03107. https://doi.org/10.1029/2007JD008503
Sorteberg, A., & Kvingedal, B. (2006). Atmospheric forcing on the Barents Sea winter ice extent. *Journal of Climate*, *19*, 4772–4784. https://doi.org/10.1175/JCLI3885.1
Sorteberg, A., & Walsh, J. E. (2008). Seasonal cyclone variability at 70°N and its impact on moisture transport into the Arctic. *Tellus*, *60A*(3), 570–586.
Sprenger, M., Fragkoulidis, G., Binder, H., Croci-Maspoli, M., Graf, P., Grams, C. M., et al. (2017). Global climatologies of Eulerian and Lagrangian flow features based on ERA-Interim. *Bulletin of the American Meteorological Society*, *98*(8), 1739–1748.

Stroeve, J., & Notz, D. (2018). Changing state of Arctic sea ice across all seasons. *Environmental Research Letters*, *13*(10), 103,001.
Tamarin, T., & Kaspi, Y. (2016). The poleward motion of extratropical cyclones from a potential vorticity tendency analysis. *Journal of the Atmospheric Sciences*, *73*(4), 1687–1707.
Tamarin-Brodsky, T., & Kaspi, Y. (2017). Enhanced poleward propagation of storms under climate change. *Nature Geoscience*, *10*(12), 908–913.
Uotila, P., Pezza, A. B., Cassano, J. J., Keay, K., & Lynch, A. H. (2009). A comparison of low pressure system statistics derived from a high-resolution NWP output and three reanalysis products over the Southern Ocean. *Journal of Geophysical Research*, *114*, D17105. https://doi.org/10.1029/2008JD011583
Vavrus, S. J. (2013). Extreme Arctic cyclones in CMIP5 historical simulations. *Geophysical Research Letters*, *40*, 6208–6212. https://doi.org/10.1002/2013GL058161
Vessey, A. F., Hodges, K. I., Shaffrey, L. C., & Day, J. J. (2020). An inter-comparison of Arctic synoptic scale storms between four global reanalysis datasets. *Climate Dynamics*, *54*, 2777–2795. https://doi.org/10.1007/s00382-020-05142-419
Vihma, T. (2014). Effects of Arctic sea ice decline on weather and climate: A review. *Surveys in Geophysics*, *35*(5), 1175–1214.
Wickström, S., Jonassen, M. O., Vihma, T., & Uotila, P. (2019). Trends in cyclones in the high-latitude North Atlantic during 1979–2016. *Quarterly Journal of the Royal Meteorological Society*, *146*, 762–779. https://doi.org/10.1002/qj.3707
Woods, C., Caballero, R., & Svensson, G. (2013). Large-scale circulation associated with moisture intrusions into the Arctic during winter. *Geophysical Research Letters*, *40*, 4717–4721. https://doi.org/10.1002/grl.50912
Yin, J. H. (2005). A consistent poleward shift of the storm tracks in simulations of 21st century climate. *Geophysical Research Letters*, *32*, L18701. https://doi.org/10.1029/2005GL023684
Zahn, M., Akperov, M., Rinke, A., Feser, F., & Mokhov, I. I. (2018). Trends of cyclone characteristics in the Arctic and their patterns from different reanalysis data. *Journal of Geophysical Research: Atmospheres*, *123*, 2737–2751. https://doi.org/10.1002/2017JD027439
Zappa, G., Pithan, F., & Shepherd, T. G. (2018). Multimodel evidence for an atmospheric circulation response to Arctic sea ice loss in the CMIP5 future projections. *Geophysical Research Letters*, *45*, 1011–1019. https://doi.org/10.1002/2017GL076096